

Activation of the S–S Bonds of Alkyl Disulfides RSSR (R = Me, Et, Pr, Buⁿ) by Heterodinuclear Phosphido-Bridged



Md. Munkir Hossain,[†] Hsiu-Mei Lin,[†] Jun Zhu,[‡] Zhenyang Lin,^{*,‡} and Shin-Guang Shyu^{*,†}

Institute of Chemistry, Academia Sinica, Taipei, Taiwan, Republic of China, and Department of Chemistry, The Hong Kong University of Science and Technology, Clear Water Bay, Kowloon, Hong Kong

Received August 9, 2005

Reactions of $\text{CpW}(\text{CO})_2(\mu\text{-PPh}_2)\text{Mo}(\text{CO})_5$ (**1**) with alkyl disulfides RSSR (R = Me, Et, Pr, Buⁿ) in refluxing dichloromethane yielded the series of new mixed-metal and mixed-ligand bridged compounds $\text{CpW}(\text{CO})(\mu\text{-SR})_2(\mu\text{-PPh}_2)\text{Mo}(\text{CO})_3$ (R = Me (**4a**), Et (**4b**), Pr (**4c**), Buⁿ (**4d**)), $\text{CpW}(\text{CO})(\mu\text{-SR})_2(\mu\text{-PPh}_2)\text{Mo}(\text{CO})(\text{SR})_2$ (R = Me (**5a**), Et (**5b**), Pr (**5c**), Buⁿ (**5d**)), and $\text{CpW}(\text{CO})(\mu\text{-SR})_2(\mu\text{-PPh}_2)\text{Mo}(\text{CO})_2(\text{PPh}_2\text{SR})$ (R = Me (**6a**), Et (**6b**), Pr (**6c**), Buⁿ (**6d**)). All except **6c** were characterized by single-crystal X-ray diffraction analysis. Formation of compounds **4–6** indicates a general procedure for cleavage of the S–S bonds of alkyl disulfides under mild conditions. Molecular structures of compounds **6a,b,d** reveal the first transformation of the bridging PPh₂ ligand of **1** to give the hybrid ligands Ph₂PSR (R = Me, Et, Buⁿ) via P–S bond formation. The average Mo–W bond distance (2.8255 Å) in the 34e dimers (**4a–d**, **6a,b,d**) is shorter than that in the 32e dimers (**5a–d**), 2.8494 Å. This appears quite unusual, according to the 18e rule. DFT calculations have been performed to investigate this unusual observation. Characterization of the substitution products $\text{CpW}(\text{CO})(\mu\text{-SMe})_2(\mu\text{-PPh}_2)\text{Mo}(\text{CO})_2\text{PPh}_2\text{Me}$ (**7**) and $\text{CpW}(\text{CO})(\mu\text{-SMe})_2(\mu\text{-PPh}_2)\text{Mo}(\text{CO})(\text{COD})$ (**8**; COD = cyclooctadiene) leads to the conclusion that carbonyl ligands on the Mo sites are more labile than those on the W sites.

Introduction

The ligating behavior of organosulfur compounds to multi-metallic sites and subsequent transformations are important in different aspects. Organic sulfides such as RSH and RSSR are the usual source of the thiolate SR ligands through activation of the S–H and S–S bonds, respectively, in the synthesis of thiolato complexes containing M–SR bonds.^{1,2} In addition, the M–SR unit can transfer the thiolate ligand to other metal centers, and thus, M–SR can act as a thiolate ligand source in the synthesis of thiolato complexes.³

A facile activation of the S–S bonds of RSSR (R = Ph, *p*-MeC₆H₄) by the reactive heterodinuclear complex $\text{CpW}(\text{CO})_2(\mu\text{-PPh}_2)\text{Mo}(\text{CO})_5$ (**1**) and formation of the 34e dimers $\text{CpW}(\text{CO})(\mu\text{-SR})_2(\mu\text{-PPh}_2)\text{Mo}(\text{CO})_3$ (R = Ph (**2a**), *p*-MeC₆H₄ (**2b**)) and the 32e dimers $\text{CpW}(\text{CO})(\mu\text{-SR})_2(\mu\text{-PPh}_2)\text{Mo}(\text{CO})(\text{SR})_2$ (R = Ph (**3a**), *p*-MeC₆H₄ (**3b**)) were reported earlier.^{5a} According to the 18e rule, a double bond should exist between the Mo and W atoms in the 32e dimer **3a**. However, the actual Mo–W bond distance (2.8589(6) Å) in **3a** is not only considerably longer than the reported Mo=W double-bond distance (2.702–2.718 Å)⁶ but also longer compared to that of the 34e dimer **2a** (2.8427(14) Å).^{5a} To verify whether such a trend is general in other 34e and 32e dimers, and to explore whether the electronic or steric effects dominate, we have prepared a series of new

34e and 32e dimers by preparing them by reactions of alkyl disulfides RSSR (with R = Me, Et, Pr, Buⁿ) with the heterodinuclear phosphido-bridged complex **1**, under mild conditions.

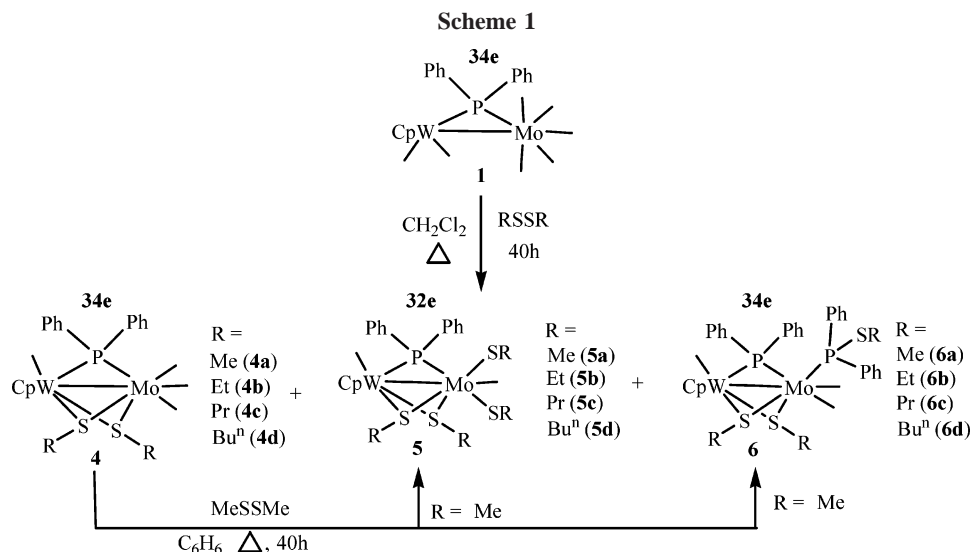
(1) (a) Treichel, P. M.; Nakagaki, P. C. *Organometallics* **1986**, *5*, 711. (b) Brandenburg, K. L.; Heeg, M. J.; Abrahamson, H. B. *Inorg. Chem.* **1987**, *26*, 1064. (c) Abrahamson, H. B.; Marxen, H. *Organometallics* **1993**, *12*, 2835. (d) Lang, R. F.; Ju, T. D.; Kiss, G.; Hoff, C. D.; Bryan, J. C.; Kubas, G. J. *J. Am. Chem. Soc.* **1994**, *116*, 7917. (e) Ahmad, M.; Bruce, R.; Knox, G. R. *J. Organomet. Chem.* **1966**, *6*, 1. (f) Watkins, D. D., Jr.; George, T. A. *J. Organomet. Chem.* **1975**, *102*, 71. (g) Havlin, R.; Knox, G. R. *Z. Naturforsch., B* **1966**, *21*, 1108. (h) Adams, R. D.; Katahira, D. A.; Yang, L. W. *Organometallics* **1982**, *1*, 235. (i) Gomes de Lima, M. B.; Guerschais, J. E.; Mercier, R.; Pétillon, F. Y. *Organometallics* **1986**, *5*, 1952. (j) Schollhammer, P.; Pétillon, F. Y.; Pichon, R.; Pöder-Guillou, S.; Talarmin, J.; Muir, K. W.; Manojlovic-Muir, Lj. *Organometallics* **1995**, *14*, 2277. (k) Liaw, W. F.; Hsieh, C.-H.; Peng, S. M.; Lee, G.-H. *Inorg. Chim. Acta* **2002**, *332*, 153 and references therein.

(2) (a) Goh, L. Y.; Tay, M. S.; Mak, T. C. W.; Wang, R.-J. *Organometallics* **1992**, *11*, 1711. (b) Aubart, M. A.; Bergman, R. G. *J. Am. Chem. Soc.* **1996**, *118*, 1793. (c) King, R. B. *J. Am. Chem. Soc.* **1963**, *85*, 1584. (d) Killips, S. D.; Knox, S. A. R. *J. Chem. Soc., Dalton Trans.* **1978**, 1260. (e) King, R. B.; Bisnette, M. B. *Inorg. Chem.* **1965**, *4*, 482. (f) Lang, R. F.; Ju, T. D.; Kiss, G.; Hoff, C. D.; Bryan, J. C.; Kubas, G. J. *Inorg. Chem.* **1994**, *33*, 3899. (g) Zanella, R.; Graziani, M. *Inorg. Chem.* **1973**, *12*, 2736. (h) Kopf, H.; Block, B. Z. *Naturforsch., B* **1966**, *21*, 1536. (i) Hainess, R. J.; Beer, J. A. D.; Greatrex, R. *J. Organomet. Chem.* **1975**, *85*, 89. (j) Lam, C. T.; Senoff, C. V. *Can. J. Chem.* **1973**, *51*, 3790. (k) Becker, E.; Mereiter, K.; Schmid, R.; Kirchner, K. *Organometallics* **2004**, *23*, 2876 and references therein.

(3) (a) Shaver, A.; Morris, S.; Turrin, R.; Day, V. W. *Inorg. Chem.* **1990**, *29*, 3622. (b) Wark, T. A.; Stephan, D. W. *Can. J. Chem.* **1990**, *68*, 565. (c) Osakada, K.; Kawaguchi, Y.; Yamamoto, T. *Organometallics* **1995**, *14*, 4542. (d) Lu, S.-W.; Okura, N.; Yoshida, T.; Otsuka, S. *J. Am. Chem. Soc.* **1983**, *105*, 7470. (e) Osakada, K.; Hataya, K.; Yamamoto, T. *Bull. Chem. Soc. Jpn.* **1998**, *71*, 2853. (f) Hossain, Md. M.; Lin, H.-M.; Shyu, S.-G. *Eur. J. Inorg. Chem.* **2001**, 2655.

[†] Academia Sinica.

[‡] The Hong Kong University of Science and Technology.



DFT calculations have been performed to examine the real cause of the increased Mo–W bond distance. Substitution of the carbonyl ligands by weak π -acceptor ligands, PPh₂Me and cyclooctadiene (COD), are also reported in this work.

Results and Discussion

A typical reaction of **1** with alkyl disulfides RSSR (R = Me, Et, Pr, Buⁿ) in refluxing dichloromethane gave compounds of the types CpW(CO)(μ -SR)₂(μ -PPh₂)Mo(CO)₃ (R = Me (**4a**), Et (**4b**), Pr (**4c**), Buⁿ (**4d**)), CpW(CO)(μ -SR)₂(μ -PPh₂)Mo(CO)₂(SR)₂ (R = Me (**5a**), Et (**5b**), Pr (**5c**), Buⁿ (**5d**)), and CpW(CO)(μ -SR)₂(μ -PPh₂)Mo(CO)₂(PPh₂SR) (R = Me (**6a**), Et (**6b**), Pr (**6c**), Buⁿ (**6d**)) (Scheme 1).

These compounds are soluble in common organic solvents. Compounds **4a–d**, **5a–d**, and **6a,b,d** were characterized by single-crystal X-ray diffraction analysis. The molecular structures of **4a–d** (Figure 1 for **4a**) show that these compounds are 34e mixed thiolato- and phosphido-bridged heterobimetallic complexes (ORTEP drawings of **4b–d**, **5b–d**, and **6b,d** are given in the Supporting Information).

Oxidative addition of RSSR to the Mo center and replacement of the CO ligands on the Mo site to form the bridging SR ligand is the most likely reaction path. Molecular structures of **5a–d** (Figure 2 for **5a**) show that these compounds are 32e heterobimetallic complexes with mixed thiolato- and phosphido-bridged ligands.

Compounds **5a–d** are the substitution products of **4a–d**, respectively, in which two carbonyl ligands on the Mo site have been replaced with two SR ligands in each case. Since the terminal SR ligands in **5a–d** are one-electron-donors, these compounds are 32e dimers with an additional Mo–W bond, as

(4) Shyu, S.-G.; Hsu, J.-Y.; Lin, P.-J.; Wu, W.-J.; Peng, S.-M.; Lee, G.-H.; Wen, Y.-S. *Organometallics* **1994**, *13*, 1699.

(5) (a) Hossain, M. M.; Lin, H. M.; Shyu, S.-G. *Organometallics* **2003**, *22*, 3262. (b) Hossain, M. M.; Lin, H. M.; Shyu, S.-G. *Organometallics* **2004**, *23*, 3941.

(6) (a) Acum, G. A.; Mays, M. J.; Raithby, P. R.; Solan, G. A. *J. Chem. Soc., Dalton Trans.* **1995**, 3049. (b) Brew, S. A.; Carr, N.; Mortimer, M. D.; Stone, F. G. A. *J. Chem. Soc., Dalton Trans.* **1991**, 811. (c) Brew, S. A.; Dosset, S. J.; Jeffery, J. C.; Stone, F. G. A. *J. Chem. Soc., Dalton Trans.* **1990**, 3709. (d) Carriedo, G. A.; Howard, J. A. K.; Jeffery, J. C.; Sneller, K.; Stone, F. G. A.; Weerasuria, A. M. M. *J. Chem. Soc., Dalton Trans.* **1990**, 953. (e) Cotton, F. A.; Eglin, J. A.; James, C. A. *Inorg. Chem.* **1993**, *32*, 687.

compared to the 34e dimers in **4a–d**, to fulfill the 18e rule. Moreover, compounds **4a–d** are the likely intermediates leading to compounds **5a–d**, respectively. Isolated **4a** did not react with an excess of MeSSMe in refluxing dichloromethane, but **4a** gave rise to **5a** in refluxing benzene (Scheme 1).

Formation of the Ph₂PSR (R = Me, Et, Pr, Buⁿ) Ligands on 6a–d. Complexes **6a,b,d** (Figure 3 for **6a**) are formed by

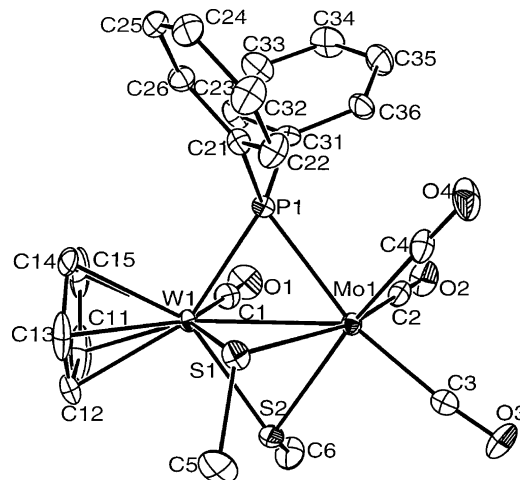


Figure 1. ORTEP drawing of **4a**, with 30% thermal ellipsoids. Hydrogen atoms are omitted.

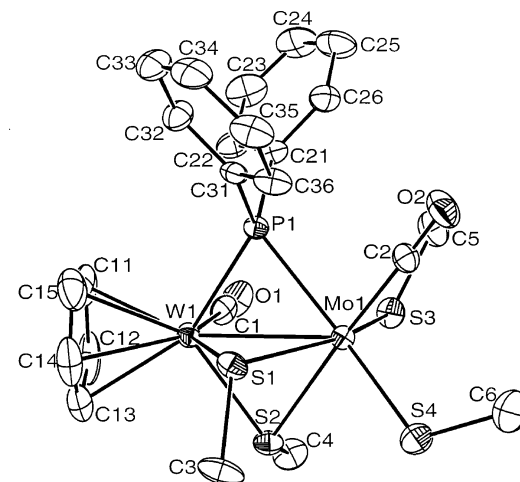


Figure 2. ORTEP drawing of **5a**, with 30% thermal ellipsoids. Hydrogen atoms are omitted.

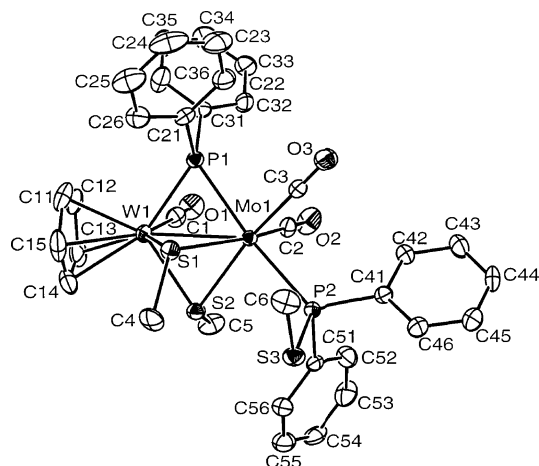


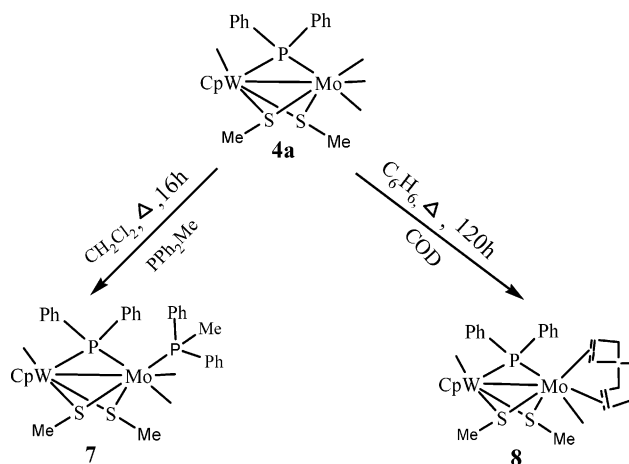
Figure 3. ORTEP drawing of **6a**, with 30% thermal ellipsoids. Hydrogen atoms are omitted.

the substitution of one CO ligand on Mo by PPh₂SR. Transformation of PPh₂ into PPh₂SR has taken place via P–S bond formation on the Mo sites, and fragmentation of the resulting products may be the source of the PPh₂SR needed in the substitution reaction, as indicated by the low yield in the formation of the complexes.

The participation of the bridging phosphido groups, in the insertion of small molecules into the M–P bonds, leads to the formation of unique bridging ligands, such as μ -R₂P=X (X = O,⁷ S,⁷ CH₂,⁸ CRR⁹), alkenyl- and butadienylphosphines,¹⁰ and diphosphines.¹¹ The coupling of the bridging phosphido ligands with CO and alkynes has been reported previously.¹² Furthermore, the versatility of the phosphido groups is shown by the reversible uptake of a hydrogen atom to form a terminal phosphine¹³ and the possibility of reversible P–C bond cleavage.¹⁴ These transformations, flexibility, and versatility of the bridging PPh₂ ligand are known, including a recent report of the interaction of a bridging PPh₂ ligand with a benzene radical to yield a PPh₃ ligand.^{5a} The formation of the PPh₂SR ligands via interaction of the bridging PPh₂ ligand and the SR fragments (from RSSR) is the subject of this paper.

In general, the thiophosphine ligands PPh₂SR are capable of undergoing intraligand thermal P–S bond cleavage and then make more bridges by reactions of the still complexed, resulting

Scheme 2



PPh₂ and SPh fragments.¹⁵ In the present work, the ligands PPh₂SR in **6a–d** are spatially terminal and are linked to the Mo sites. This is the most likely configuration, as the complexes **6a–d** are already overcrowded by the SR and PPh₂ bridges. Formation of the complexes **6a–d** was not observed during reactions between **1** and aryl disulfides ArSSAr (Ar = Ph, *p*-MeC₆H₄) under identical conditions.^{5a} This indicates the lack of availability of the PPh₂SAr ligands for complexation. This may be due to two reasons. First, the reaction paths, which are followed by alkyl disulfides to react with the phosphido-bridging PPh₂ ligand in **1** to form PPh₂SR, are not favorable for aryl disulfides to give PPh₂SAr. Second, the PPh₂SAr ligands formed by following paths similar to those for dialkyl disulfides or even different paths might have been fragmented to PPh₂ and SAr¹⁵ under identical conditions, since the P–SAr bond is weaker than the P–SR bond (R = alkyl).¹⁶

Reactions of 4a with PPh₂Me and COD. When a dichloromethane solution of **4a** was heated at reflux for 16 h with PPh₂Me, compound **7** was obtained. The benzene solution of **4a**, when heated at reflux with COD for a much longer time (120 h), gave compound **8** (Scheme 2).

The MoWPS₂ cores of **7** and **8** have geometries (Figures 4 and 5) similar to that of **4a**. In principle, both **7** and **8** are substitution products of **4a**, where carbonyl ligands on the Mo site are replaced with PPh₂Me and COD, respectively. Carbonyl ligands are π -acceptors. Due to the high oxidation state of Mo in **4a**, the availability of electron density on the Mo site for back-donation to the carbonyl ligands is reduced. As a consequence, the Mo–C bond is weakened compared to the W–C bond, since the W site is attached to the π -donor cyclopentadienyl ring. This makes the carbonyl ligands on the Mo site more labile than those on the W site.

X-ray Structures of Compounds 4a–d, 5a–d, 6a,b,d, 7, and 8. Molecular structures of **4a–d**, **5a–d**, **6a,b,d**, **7**, and **8** have been determined by single-crystal X-ray diffraction analyses. The experimental data and the selected bond distances and bond angles are summarized in the Supporting In-

- (7) Klingert, B.; Werner, H. *J. Organomet. Chem.* **1983**, *252*, C47.
 (8) (a) Yu, Y.-F.; Chau, C.-N.; Wojcicki, A.; Calligaris, M.; Nardin, G.; Balducci, G. *J. Am. Chem. Soc.* **1984**, *106*, 3704. (b) Yu, Y.-F.; Chau, Gallucci, J.; Wojcicki, A. *J. Chem. Soc., Chem. Commun.* **1984**, 653. (c) Rosenberg, S.; Whittle, R. R.; Geoffroy, G. L. *J. Am. Chem. Soc.* **1984**, *106*, 5934. (d) Rosenberg, S.; Geoffroy, G. L.; Rheingold, A. L. *Organometallics* **1985**, *4*, 1184. (e) Geoffroy, G. L.; Rosenberg, S.; Shulman, P. M.; Whittle, R. R. *J. Am. Chem. Soc.* **1984**, *106*, 1519.
 (9) (a) Werner, H.; Zolk, R. *Organometallics* **1985**, *4*, 601. (b) Werner, H.; Zolk, R. *Chem. Ber.* **1987**, *120*, 1003.
 (10) (a) Horton, A. D.; Mays, M. J.; Raithby, P. R. *J. Chem. Soc., Chem. Commun.* **1985**, 247. (b) Henrick, K.; Iggo, J. A.; Mays, M. J.; Raithby, P. R. *J. Chem. Soc., Chem. Commun.* **1984**, 209.
 (11) Yu, Y.-F.; Wojcicki, A.; Calligaris, M.; Nardin, G. *Organometallics* **1986**, *5*, 47.
 (12) (a) Regragui, R.; Dixneuf, P. H.; Taylor, N. J.; Carty, A. J. *Organometallics* **1984**, *3*, 814. (b) Regragui, R.; Dixneuf, P. H.; Taylor, N. J.; Carty, A. J. *Organometallics* **1990**, *9*, 2234.
 (13) (a) Lukan, N.; Lavigne, G.; Bonnet, J.-J.; Reau, R.; Neibecker, D.; Tkatchenko, I. *J. Am. Chem. Soc.* **1988**, *110*, 5369. (b) Livotto, F. S.; Vargas, M. D.; Braga, D.; Grepioni, F. *J. Chem. Soc., Dalton Trans.* **1992**, 577. (c) Livotto, P. S.; Raithby, P. R.; Vargas, M. *J. Chem. Soc., Dalton Trans.* **1993**, 1797.
 (14) (a) Gastel, F. V.; Maclaughlin, S. A.; Lynch, M.; Carty, A. J.; Sappa, E.; Tiripicchio, A.; Camellini, M. T. *J. Organomet. Chem.* **1987**, *326*, C65. (b) Cabeza, J. A.; Rio, I. D.; Riera, V.; Garcia-Granda, S.; Sanni, S. B. *Organometallics* **1997**, *16*, 1743.

- (15) (a) Job, B. A.; McLean, R. N. A.; Thompson, D. T. *J. Chem. Soc., Chem. Commun.* **1966**, 895. (b) Edwards, A. J.; Martin, A.; Mays, M. J.; Raithby, P. R.; Solan, G. A. *J. Chem. Soc., Chem. Commun.* **1992**, 1416. (c) Martin, A.; Mays, M. J.; Raithby, P. R.; Solan, G. A. *J. Chem. Soc., Dalton Trans.* **1993**, 1431. (d) Conole, G.; Kessler, M. K.; Mays, M. J.; Pateman, G. E.; Solan, G. A. *Polyhedron* **1998**, *17*, 2993. (e) King, G. D.; Mays, M. J.; Pateman, G. E.; Raithby, P. R.; Rennie, M. A.; Solan, G. A.; Choi, N.; Conole, G.; McPartlin, M. *J. Chem. Soc., Dalton Trans.* **1999**, 4447.
 (16) Bentrude, W. G.; Kawashima, T.; Keys, B. A.; Garroussian, M.; Heide, W.; Wedegaertner, D. A. *J. Am. Chem. Soc.* **1987**, *109*, 1227.

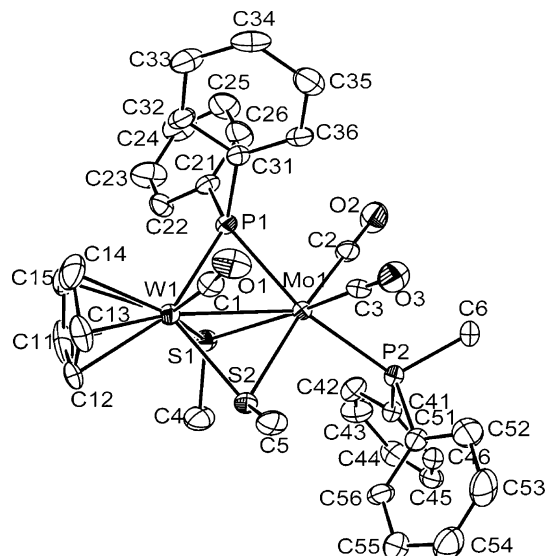


Figure 4. ORTEP drawing of **7**, with 30% thermal ellipsoids. Hydrogen atoms are omitted.

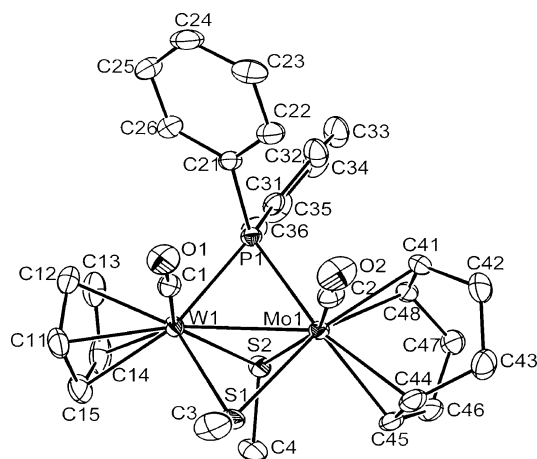
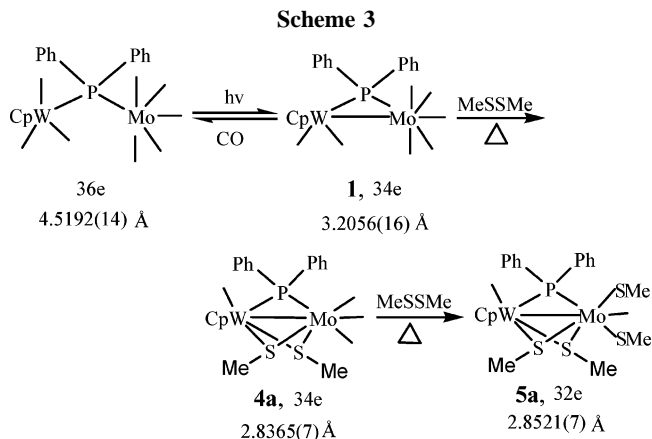


Figure 5. ORTEP drawing of **8**, with 30% thermal ellipsoids. Hydrogen atoms are omitted.

formation.^{17a,b} The relevant bond lengths such as Mo–W, Mo_{br}–S, Mo_{ter}–S, Mo_{br}–P, W_{br}–S, and W_{br}–P and average values of the acute angles (M–X–M, X = S, P) of **4a–d**, **5a–d**, **6a,b,d**, **7**, and **8** are given in Table 1.

The average Mo–W bond lengths of **4a–d**, **5a–d**, **6a,b,d**, **7**, and **8** are shorter by 0.424 Å as compared to the Mo–W (3.2054(16) Å) bond length in the parent compound **1**. The



shortening of the Mo–W bond distance in compounds **4a–d**, **5a–d**, **6a,b,d**, **7**, and **8** is expected, since the number of bridges between the Mo and W sites is increased compared to that in the parent compound **1**.^{5b}

The bonding of Mo to the terminal sulfur atoms in **5a–d** does not follow a predictable trend (Table 1). The Mo_{ter}–S bonds (2.3680 Å (av)) trans to the phosphido bridging ligand and the Mo_{ter}–S bonds (2.301 Å (av)) trans to the thiolato bridging ligand differ by 0.067 Å in bond distances. This may be due to the trans influence of the bridging PPh₂ ligand. Furthermore, the Mo_{ter}–S distances (2.3345 Å (av)) observed in **5a–d** are shorter by 0.1155 Å than the normal single Mo–S bond (2.45 Å), which is calculated from Slater's radii.¹⁸ However, they are clearly in the range observed for Mo_{ter}–S^{17c} single-bond distances, which is 2.2335–2.579 Å. The shorter Mo_{ter}–S bond distances compared to the calculated normal Mo–S single-bond distances can be attributed to the existence of Mo–S π -bonding. Thus, the shorter Mo_{ter}–S distances in **5a–d** confirm the existence of the π -bonding between molybdenum and sulfur atoms.

The 18e Rule and the Metal–Metal Bond Distances in 34e and 32e Dimers. Scheme 3 presents a sequence of metal–metal bond distance variation in heterobimetallic mixed thiolato- and phosphido-bridged complexes. The conversion of the monophosphido-bridged 34e dimer **1** into the 34e triply bridged **4a** reduces the Mo–W bond distance by 0.3689 Å. This is due to the increase in the number of bridges between the Mo and W in **4a**.^{5b} However, the Mo–W bond distance (2.8521(7) Å) in the triply bridged 32e dimer (**5a**) is not only considerably longer than reported Mo=W double bonds (2.702–2.718)⁶ but also longer compared to the distance in the 34e dimer **4a**. This is apparently unusual according to the 18e rule.

Table 1. Relevant Bond Distances and Acute Angles of Compounds 4a–d, 5a–d, 6a,b,d, 7, and 8

compd	Mo–W (Å)	Mo _{ter} –S (av) (Å)	Mo _{br} –S (av) (Å)	W _{br} –S (av) (Å)	Mo _{br} –P (Å)	W _{br} –P (Å)	M–X–M (av) (deg)
CpW(CO)(μ -SMe) ₂ (μ -PPh ₂)Mo(CO) ₃ (34e) (4a)	2.8365(7)		2.5570	2.4732	2.4674(15)	2.3860(15)	70.13
CpW(CO)(μ -SEt) ₂ (μ -PPh ₂)Mo(CO) ₃ (34e) (4b)	2.8348(2)		2.5463	2.4727	2.4684(6)	2.3832(6)	69.67
CpW(CO)(μ -SPr) ₂ (μ -PPh ₂)Mo(CO) ₃ (34e) (4c)	2.8249(8)		2.5445	2.4695	2.490(2)	2.388(2)	69.29
CpW(CO)(μ -S ⁿ Bu) ₂ (μ -PPh ₂)Mo(CO) ₃ (34e) (4d)	2.8348(11)		2.5520	2.4680	2.488(3)	2.381(4)	69.56
CpW(CO)(μ -SMe) ₂ (μ -PPh ₂)Mo(CO)(SMe) ₂ (32e) (5a)	2.8521(7)	2.3365	2.5475	2.4534	2.499(2)	2.3869(18)	69.59
CpW(CO)(μ -SEt) ₂ (μ -PPh ₂)Mo(CO)(SEt) ₂ (32e) (5b)	2.8488(8)	2.3385	2.5570	2.4611	2.494(2)	2.389(2)	69.88
CpW(CO)(μ -SPr) ₂ (μ -PPh ₂)Mo(CO)(SPr) ₂ (32e) (5c)	2.8511(6)	2.3313	2.5606	2.4579	2.496(17)	2.3916(17)	69.91
CpW(CO)(μ -S ⁿ Bu) ₂ (μ -PPh ₂)Mo(CO)(S ⁿ Bu) ₂ (32e) (5d)	2.8458(5)	2.3326	2.5609	2.4630	2.488(12)	2.3874(12)	69.78
CpW(CO)(μ -SMe) ₂ (μ -PPh ₂)Mo(CO) ₂ (PPh ₂ SMe) (34e) (6a)	2.8230(6)		2.5656	2.4625	2.4726(15)	2.3957(16)	69.15
CpW(CO)(μ -SEt) ₂ (μ -PPh ₂)Mo(CO) ₂ (PPh ₂ SEt) (34e) (6b)	2.8018(9)		2.5506	2.4787	2.4512(19)	2.391(2)	68.70
CpW(CO)(μ -S ⁿ Bu) ₂ (μ -PPh ₂)Mo(CO) ₂ (PPh ₂ S ⁿ Bu) (34e) (6d)	2.8226(5)		2.5567	2.4856	2.4411(15)	2.3925(15)	69.19
CpW(CO)(μ -SMe) ₂ (μ -PPh ₂)Mo(CO) ₂ (PPh ₂ Me) (34e) (7)	2.8028(13)		2.5615	2.4805	2.449(2)	2.396(3)	68.57
CpW(CO)(μ -SMe) ₂ (μ -PPh ₂)Mo(CO)(COD) (34e) (8)	2.8338(9)		2.5342	2.4670	2.4752(11)	2.4142(11)	69.62

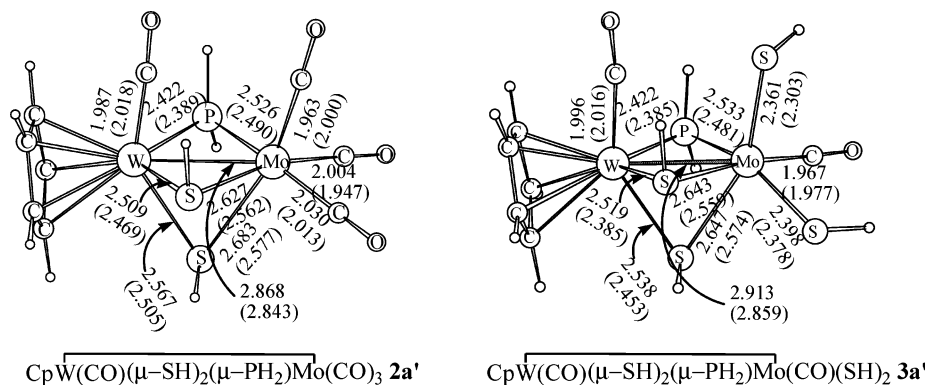


Figure 6. Selected structural parameters (bond lengths in Å) calculated for the model complexes together with experimental structural parameters for **2a** and **3a** shown in parentheses.

We know that the metal–metal bond distances in these dinuclear compounds are influenced by several parameters, such as coordination numbers of the metal atoms as well as the geometry of the M_2S_2 core.¹⁹ The compounds **4a** and **5a** are similar with respect to the ligand coordination (similar core $WMoS_2P$) and the number of bridges (1 P and 2 S). They differ only in the number of valence electrons due to substitution of two two-electron-donor carbonyl ligands by the oxidative addition of two one-electron-donor terminal SMe ligands. Although the formal oxidation states of Mo and W are changed in **5a**, the type of substituents attached to them should be the dominant factor in determining the resulting bond distance.²⁰ The steric effect of the alkyl group is excluded, as a similar trend is also observed in other 32e and 34e dimers with SR bonding where R is relatively bulky (R = Et, Pr, Buⁿ, Ph^{5a}) (Table 1). Moreover, this trend not only is observed in the case of the Mo–W dimers but also has been reported for Mo–Mo distances in 32e $Cp(CO)Mo(\mu-SPh)_3Mo(CO)(SPh)_2$ (2.8040–(9) Å) and 34e $Cp(CO)Mo(\mu-SCH_2Ph)_3Mo(CO)_3$ dimers (2.779–(4) Å).²¹ Thus, the trend of increasing the metal–metal bond distance in the 32e dimers compared to the 34e dimers may be electronic in nature. DFT calculations have been performed in order to examine the possible explanations.

DFT Calculations. Crystal structure analysis indicates that the Mo–W bond distance (2.843 Å) in **2a** is shorter than that (2.859 Å) in **3a**.^{5a} According to the 18e rule, the Mo–W bonds in **2a** and **3a** should correspond to a single and double bond, respectively. The metal–metal double bond in **3a** is unexpectedly longer than the metal–metal single bond in **2a**. To better understand the nature of the Mo–W bonding interactions in the two compounds, we carried out molecular orbital calculations at the B3LYP level of density functional theory. In the model compounds (**2a'** and **3a'**), hydrogen atoms were used to replace the phenyl groups of the phosphine and thiolate ligands in our calculations. The important structural parameters calculated for the two model compounds are shown in Figure 6, together with those from the experimentally characterized compounds **2a** and **3a**.

Figure 6 shows that the theoretical calculations accurately reproduce the experimental results, in which the formally

double-bond Mo–W distance in **3a** is longer than the formally single-bond Mo–W distance in **2a**. To provide a reasonable explanation for the unusual observation, we hypothesize that the terminal Mo–S bonds in **3a** may have a double-bond character as a result of the $S(p_\pi) \rightarrow Mo(d)$ ligand-to-metal dative π -bonding interactions. Indeed, the natural bond orbital (NBO) analysis²² indicates that the Wiberg bond indices (bond orders),²³ which are a measure of bond strength, calculated for the terminal Mo–S bonds (0.95 and 1.01) are more than twice those calculated for the bridging Mo–S bonds (0.37 and 0.40). The π -bonding interactions between Mo and the terminal thiolate ligands imply that the Mo–W bond in **3a** is not a real double bond, because the terminal thiolate ligands provide π -electrons for bonding with the Mo center.

To test the hypothesis mentioned above, we calculated a new model compound, $CpW(CO)(\mu-SPh)_2(\mu-PPh_2)Mo(CO)Cl_2$ (**3a''**), in which two chloride ligands were used to replace the two terminal thiolate ligands in **3a**. Due to their greater electronegativity, the chloride ligands are expected to have weaker π -bonding ability in comparison to the thiolate ligands. As expected, the Mo–W bond distance (2.892 Å) calculated for **3a''** is shorter than that (2.913 Å) calculated for **3a'** due to the weaker π -donating ability of the Cl ligands. To further confirm the hypothesis, we calculated another model compound, $CpW(CO)(\mu-SPh)_2(\mu-PPh_2)Mo(CO)\{S(O)H\}_2$ (**3a'''**), using $-S(O)H$ as the terminal ligands, and found that the Mo–W bond length in **3a'''** is significantly reduced to 2.854 Å, not only shorter than that (2.913 Å) in **3a'** but also shorter than that (2.868 Å) in **2a'**. Introduction of the oxo group in the $-S(O)H$ ligands further decreases the π -donating ability of the terminal ligands. In **3a'''**, it is interesting to note that one of the $-S(O)H$ ligands is coplanar with Mo, indicating a π -dative bond with the Mo center. When we constrained the two terminal $-S(O)H$ ligands to adopt pyramidal structures, the Mo–W bond distance becomes the shortest (2.837 Å), as the pyramidal terminal $-S(O)H$ ligands are incapable of donating their lone-pair electrons to the Mo center and a real $Mo=W$ double bond is formed. Therefore, although the Mo–W bond in **3a** is formally a double bond according to the 18e rule, the bond strength has been significantly weakened, due to the π -donation of the terminal thiolate ligand. This is also supported by the observed shorter $Mo_{ter}-S$ bond distances in 32e dimers compared to 34e dimers (Table 1).

(17) In the Supporting Information: (a) see Tables 1Sa, 1Sb, and 1Sc for experimental data; (b) see Tables 2Sa, 2Sb, 2Sc, and 2Sd for the selected bond distances and bond angles; (c) see Table 3S for $Mo_{ter}-S$ bond distances for a few mononuclear and binuclear molybdenum complexes.

(18) Slater, J. C. *J. Chem. Phys.* **1964**, *41*, 3199.

(19) Kuhn, N.; Zauder, E.; Boses, R.; Blaser, D. *J. Chem. Soc., Dalton Trans.* **1988**, 2171.

(20) Stevenson, D. L.; Dahl, L. F. *J. Am. Chem. Soc.* **1967**, *89*, 3721.

(21) Dickson, R. S.; Fallon, G. D.; Jackson, W. R.; Polas, A. J. *Organomet. Chem.* **2000**, *607*, 156.

(22) Glendening, E. D.; Reed, A. E.; Carpenter, J. E.; Weighold, F. NBO, Version 3.1.

(23) Wiberg, K. B. *Tetrahedron* **1968**, *24*, 1083.

Experimental Section

General Procedures. General procedures were the same as those described in detail in the earlier work.^{5a}

Reaction of 1 with Me₂S₂. To a dichloromethane solution (75 mL) of **1** (500 mg, 0.69 mmol) was added Me₂S₂ (260 mg, 2.76 mmol), and the mixture was heated at reflux for about 40 h. The reaction mixture was evaporated to dryness. The residue was dissolved in dichloromethane (10 mL), and the solution was subjected to chromatographic separation using a silica gel column. Two fractions were collected by elution with hexane and dichloromethane (6:4), and the third fraction was collected using neat dichloromethane. Evaporation of the first dirty green fraction gave compound **4a**. The second brown fraction was identified as compound **6a**. The third reddish orange fraction afforded compound **5a** after evaporation of the solvent. **4a**: yield 208 mg, 41%. Anal. Calcd for C₂₃H₂₁O₄PS₂MoW: C, 37.50; H, 2.85. Found: C, 37.54; H, 2.52. IR (CH₂Cl₂): $\nu(\text{CO})$ 1992 (vs), 1960 (s), 1922 (m), 1845 (s) cm⁻¹. ¹H NMR (CDCl₃): δ 7.62–7.21 (m, 10H, C₆H₅), 5.63 (s, 5H, C₅H₅), 2.45 (s, 3H, CH₃), 1.39 (s, 3H, CH₃). ³¹P{¹H} NMR (CH₂Cl₂): δ 132.5 (s). **6a**: yield 45 mg, 7%. Anal. Calcd for C₃₅H₃₄O₃P₂S₃MoW: C, 44.68; H, 3.62. Found: C, 44.62; H, 3.31. IR (CH₂Cl₂): $\nu(\text{CO})$ 1951 (vs), 1908 (vs), 1809 (vs) cm⁻¹. ¹H NMR (CDCl₃): δ 7.48–7.19 (m, 20H, C₆H₅), 5.50 (s, 5H, C₅H₅), 1.91 (s, 3H, CH₃), 1.88 (s, 3H, CH₃), 1.61 (s, 3H, CH₃). ³¹P{¹H} NMR (CH₂Cl₂): δ 125.7 (d), 75.6 (d, ²J_{P–P} = 31.10 Hz). **5a**: yield 32 mg, 6%. Anal. Calcd for C₂₃H₂₇O₂PS₄MoW: C, 35.66; H, 3.49. Found: C, 35.72; H, 3.61. IR (CH₂Cl₂): $\nu(\text{CO})$ 1971 (s), 1885 (s) cm⁻¹. ¹H NMR (CDCl₃): δ 7.61–7.26 (m, 10H, C₆H₅), 5.50 (s, 5H, C₅H₅), 2.81 (s, 3H, CH₃), 2.55 (s, 3H, CH₃), 2.43 (s, 3H, CH₃), 2.18 (s, 3H, CH₃). ³¹P{¹H} NMR (CH₂Cl₂): δ 140.5 (s).

Reactions of 1 with RSSR (R = Et, Pr, Buⁿ). To a dichloromethane solution (75 mL) of **1** (500 mg, 0.69 mmol) was added Et₂S₂ (336 mg, 2.76 mmol), and the mixture was kept at reflux for 40 h and then concentrated to 10 mL. Silica gel chromatographic separation using hexane and dichloromethane (6:4) gave compounds **4b**, **6b**, and **5b** as the first dirty green, second brown, and third reddish orange bands, respectively. **4b**: yield 211 mg, 40%. Anal. Calcd for C₂₅H₂₅O₄PS₂MoW: C, 39.26; H, 3.27. Found: C, 38.88; H, 3.09. IR (CH₂Cl₂): $\nu(\text{CO})$ 1991 (vs), 1959 (s), 1922 (m), 1846 (s) cm⁻¹. ¹H NMR (CDCl₃): δ 7.61–7.22 (m, 10H, C₆H₅), 5.62 (s, 5H, C₅H₅), 2.79 (m, 1H), 2.55 (m, 1H), 2.09 (m, 1H), 1.71 (m, 1H), 1.37 (t, 3H, CH₃), 0.87 (t, 3H, CH₃). ³¹P{¹H} NMR (CH₂Cl₂): δ 131.2 (s). **6b**: yield 61 mg, 9%. Anal. Calcd for C₃₈H₄₀O₃P₂S₃MoW: C, 46.44; H, 4.07. Found: C, 46.05; H, 3.75. IR (CH₂Cl₂): $\nu(\text{CO})$ 1948 (vs), 1906 (vs), 1809 (vs) cm⁻¹. ¹H NMR (CDCl₃): δ 7.53–7.21 (m, 20H, C₆H₅), 5.57 (s, 5H, C₅H₅), 2.85 (m, 1H), 2.48 (m, 1H), 2.31 (m, 1H), 2.22 (m, 1H), 1.84 (m, 1H), 1.65 (m, 1H), 1.07 (t, 3H, CH₃), 1.09 (t, 3H, CH₃), 0.71 (t, 3H, CH₃). ³¹P{¹H} NMR (CH₂Cl₂): δ 123.3 (d), 69.9 (d, ²J_{P–P} = 30.29 Hz). **5b**: yield 50 mg, 9%. Anal. Calcd for C₂₇H₃₅O₂PS₄MoW: C, 39.04; H, 4.22. Found: C, 38.89; H, 3.90. IR (CH₂Cl₂): $\nu(\text{CO})$ 1968 (s), 1879 (s) cm⁻¹. ¹H NMR (CD₂Cl₂): δ 7.99–7.16 (m, 10H, C₆H₅), 5.56 (s, 5H, C₅H₅), 3.61 (m, 1H), 3.42 (m, 1H), 3.25 (m, 1H), 2.89 (m, 1H), 2.76 (m, 1H), 2.63 (m, 1H), 2.39 (m, 1H), 2.04 (m, 1H), 1.43 (m, 6H, CH₃), 1.02 (t, 3H, CH₃), 0.91 (t, 3H, CH₃). ³¹P{¹H} NMR (CH₂Cl₂): δ 138.3 (s).

The typical reactions of the disulfides RSSR (R = Pr (414 mg, 2.76 mmol) and Buⁿ (767 mg, 2.76 mmol)) with **1** (500 mg, 0.69 mmol in each case) and their workup produced the respective compounds **4c**, **5c**, **6c** and **4d**, **5d**, **6d**.

For Pr₂S₂, data for the compounds obtained are as follows. First dirty green band **4c**: yield 175 mg, 32%. Anal. Calcd for C₂₇H₂₉O₄PS₂MoW: C, 40.91; H, 3.66. Found: C, 41.25; H, 3.42. IR (CH₂Cl₂): $\nu(\text{CO})$ 1990 (vs), 1959 (s), 1921 (m), 1845 (s) cm⁻¹. ¹H NMR (CDCl₃): δ 7.66–7.25 (m, 10H, C₆H₅), 5.64 (s, 5H, C₅H₅), 2.80 (m, 1H), 2.56 (m, 1H), 2.14 (m, 1H), 1.77 (m, 2H), 1.68 (m, 1H), 1.23 (m, 2H), 1.07 (s, CH₃), 0.79 (t, 3H, CH₃). ³¹P{¹H} NMR (CH₂Cl₂): δ 131.4 (s). Second brown band **6c**: yield 83 mg, 12%. Anal. Calcd for C₄₁H₄₆O₃P₂S₃MoW: C, 48.05; H, 4.49. Found: C, 47.92; H, 4.52. IR (CH₂Cl₂): $\nu(\text{CO})$ 1948 (vs), 1905 (vs), 1809 (vs) cm⁻¹. ¹H NMR (CDCl₃): δ 7.54–7.11 (m, 20H, C₆H₅), 5.54 (s, 5H, C₅H₅), 2.79 (m, 1H), 2.44 (m, 1H), 2.28 (m, 1H), 1.66 (m, 4H), 1.42 (m, 2H), 1.26 (m, 3H), 0.078 (m, 6H, CH₃), 0.65 (t, 3H, CH₃). ³¹P{¹H} NMR (CH₂Cl₂): δ 123.6 (d), 70.6 (d, ²J_{P–P} = 30.37 Hz). Third reddish orange band **5c**: yield 31 mg, 5%. Anal. Calcd for C₃₁H₄₃O₂PS₄MoW: C, 41.99; H, 4.85. Found: C, 41.83; H, 4.74. IR (CH₂Cl₂): $\nu(\text{CO})$ 1960 (s), 1874 (s) cm⁻¹. ¹H NMR (CDCl₃): δ 7.60–7.27 (m, 10H, C₆H₅), 5.51 (s, 5H, C₅H₅), 3.57 (m, 1H), 3.28 (m, 1H), 3.13 (m, 1H), 2.70 (m, 1H), 2.51 (m, 4H), 2.52 (m, 1H), 1.80 (m, 2H), 1.75 (m, 2H), 1.42 (m, 2H), 1.26 (m, 1H), 1.11 (t, 3H, CH₃), 1.00 (q, 3H, CH₃), 0.80 (t, 3H, CH₃), 0.66 (t, 3H, CH₃). ³¹P{¹H} NMR (CH₂Cl₂): δ 138.8 (s).

For Buⁿ₂S₂, data for the compounds obtained are as follows. First dirty green band **4d**: yield 232 mg, 41%. Anal. Calcd for C₂₉H₃₃O₄PS₂MoW: C, 42.44; H, 4.02. Found: C, 42.72; H, 3.65. IR (CH₂Cl₂): $\nu(\text{CO})$ 1990 (vs), 1958 (s), 1921 (m), 1845 (s) cm⁻¹. ¹H NMR (CDCl₃): δ 7.65–7.25 (m, 10H, C₆H₅), 5.63 (s, 5H, C₅H₅), 2.85 (m, 1H), 2.58 (m, 1H), 2.15 (m, 1H), 1.72 (m, 3H), 1.50 (m, 2H), 1.19 (m, 4H), 0.94 (t, 3H, CH₃), 0.82 (t, 3H, CH₃). ³¹P{¹H} NMR (CH₂Cl₂): δ 131.5 (s). Second brown band **6d**: yield 59 mg, 8%. Anal. Calcd for C₄₄H₅₂O₃P₂S₃MoW: C, 49.53; H, 4.88. Found: C, 49.47; H, 4.92. IR (CH₂Cl₂): $\nu(\text{CO})$ 1948 (vs), 1905 (vs), 1809 (vs) cm⁻¹. ¹H NMR (CDCl₃): δ 8.04–7.22 (m, 20H, C₆H₅), 5.54 (s, 5H, C₅H₅), 2.45 (m, 1H), 2.29 (m, 1H), 2.18 (m, 1H), 1.72 (m, 2H), 1.52 (m, 1H), 1.38 (m, 2H), 1.18 (m, 6H), 1.01 (m, 3H), 0.91 (m, 1H), 0.79 (m, 3H, CH₃), 0.71 (m, 6H, CH₃). ³¹P{¹H} NMR (CH₂Cl₂): δ 123.6 (d), 70.6 (d, ²J_{P–P} = 30.33 Hz). Third reddish orange band **5d**: yield 72 mg, 11%. Anal. Calcd for C₃₅H₅₁O₂PS₄MoW: C, 44.55; H, 5.41. Found: C, 44.87; H, 5.20. IR (CH₂Cl₂): $\nu(\text{CO})$ 1968 (s), 1877 (s) cm⁻¹. ¹H NMR (CDCl₃): δ 7.72–7.20 (m, 10H, C₆H₅), (d, 5H, C₅H₅), 3.61 (m, 1H), 3.47 (m, 1H), 3.26 (m, 1H), 2.94 (m, 1H), 2.72 (m, 2H), 2.40 (m, 1H), 1.77 (m, 3H), 1.66 (m, 1H), 1.52 (m, 3H), 1.41 (m, 3H), 1.27 (m, 4H), 1.07 (m, 3H), 0.95 (m, 6H, CH₃), 0.85 (q, 3H, CH₃), 0.72 (q, 3H, CH₃). ³¹P{¹H} NMR (CH₂Cl₂): δ 138.6 (s).

Reaction of PPh₂Me with 4a. To a dichloromethane solution (50 mL) of **4a** (100 mg, 0.13 mmol) was added PPh₂Me (52 mg, 0.26 mmol), and the mixture was heated at reflux for 16 h. After concentration to 5 mL, silica gel chromatography using hexane and dichloromethane (50:50) isolated **7** as a brown band. Yield: 97 mg, 82%. Anal. Calcd for C₃₅H₃₄O₃P₂S₂MoW: C, 46.25; H, 3.74. Found: C, 46.35; H, 3.74. IR (CH₂Cl₂): $\nu(\text{CO})$ 1947 (vs), 1906 (vs), 1802 (vs) cm⁻¹. ¹H NMR (CDCl₃): δ 7.69–7.22 (m, 20H, C₆H₅), 5.58 (s, 5H, C₅H₅), 2.39 (d, 3H, CH₃, ²J_{P–H} = 6.71), 1.68 (s, 3H, CH₃), 1.03 (s, 3H, CH₃). ³¹P{¹H} NMR (CH₂Cl₂): δ 122.2 (d), 25.5 (d, ²J_{P–P} = 24.59 Hz).

Reaction of COD with 4a. To a benzene solution (50 mL) of **4a** (200 mg, 0.27 mmol) was added cyclooctadiene (290 mg, 2.7 mmol), and the mixture was heated at reflux for 120 h. The solution was then evaporated to dryness, and the residue was dissolved in 5 mL of dichloromethane. Silica gel chromatography using hexane and dichloromethane (50:50) isolated compound **8** as a second orange band. The first dirty green band was unreacted **4a** (30 mg). **8**: yield 41 mg, 23%. Anal. Calcd for C₂₉H₃₃O₂PS₂MoW: C, 44.16; H, 4.18. Found: C, 44.07; H, 4.10. IR (CH₂Cl₂): $\nu(\text{CO})$ 1933 (vs), 1841 (s) cm⁻¹. ¹H NMR (CDCl₃): δ 7.55–7.09 (m, 10H, C₆H₅), 5.56 (s, 5H, C₅H₅), 5.05 (m, 1H), 4.77 (m, 1H), 4.63 (m, 1H), 3.33 (m, 1H), 2.93 (m, 2H), 2.59 (m, 2H), 2.35 (s, 6H, CH₃), 2.10 (m, 2H), 1.98 (m, 2H). ³¹P{¹H} NMR (CH₂Cl₂): δ 75.8 (s). The yield is calculated on the basis of reacted **4a**.

Reaction of 4a with Me₂S₂ in Dichloromethane. To a dichloromethane solution (50 mL) of **4a** (200 mg, 0.27 mmol) was added Me₂S₂ (101 mg, 1.1 mmol), and the mixture was heated at reflux for 40 h. After concentration to 5 mL, silica gel column chroma-

tography using hexane and dichloromethane (50:50) recovered unreacted **4a** in 97% yield (97 mg).

Reaction of 4a with Me₂S₂ in Benzene. To a benzene solution (50 mL) of **4a** (200 mg, 0.27 mmol) was added Me₂S₂ (101 mg, 1.1 mmol), and the mixture was heated at reflux for 40 h. After concentration to 5 mL, silica gel column chromatography using hexane and dichloromethane (50:50) recovered unreacted **4a** (25 mg, 12.5%) and **6a** (25 mg, 11%) as the first dirty green and the second brown bands, respectively, and then isolated **5a** (6 mg, 3%) using neat dichloromethane. The yield is calculated on the basis of reacted **4a**.

Crystal Structure Determination of 4a–d, 5a–d, 6a,b,d, 7, and 8. The single crystals of **4a,b,d**, **5a,b**, **6a**, and **8** for X-ray diffraction analyses were grown by slow evaporation of their respective dichloromethane solutions layered with hexane, whereas slow evaporation of the dichloromethane solutions of **5d** and **7** layered with toluene, of **5c** and **6b,d** layered with acetonitrile, and of **4c** layered with THF produce their respective X-ray-quality crystals at 0 °C. Crystals of all compounds were mounted on a glass fiber. Data collections were performed with Mo K α radiation ($\lambda = 0.71073$ Å) on Nonius KappaCCD and Enraf-Nonius CAD4 diffractometers.^{17a} Cell parameters were refined from 25 reflections on an Enraf-Nonius CAD4 diffractometer. The unit-cell parameters were obtained by a least-squares fit to the automatically centered settings for reflections on the Nonius KappaCCD diffractometer. Intensity data were collected by using the $\omega/2\theta$ scan mode. Corrections were made for Lorentz and polarization effects. The structures were solved by direct methods (SHELX-97).²⁴ All non-hydrogen atoms were located from the difference Fourier maps and were refined by full-matrix least-squares procedures. Hydrogen atoms were calculated and refined with an overall isotropic temperature factor. Calculations and full-matrix least-squares refinements were performed utilizing the WINGX program package²⁵ in the evaluation of values of $R(F_o)$ for reflections with $I > 2\sigma(I)$ and $R_w(F_o)$, where $R = \sum||F_o| - |F_c||/\sum|F_o|$ and $R_w = [\sum\{w(F_o^2 - F_c^2)^2\}/\sum\{w(F_o^2)^2\}]^{1/2}$. Intensities were corrected for absorption.

Computational Details. Molecular geometries were optimized at the Becke3LYP (B3LYP) level of density functional theory.²⁶

(24) Sheldrick, G. M. *SHELXL-97*; University of Göttingen, Göttingen, Germany, 1997.

(25) Farrugia, L. J. *J. Appl. Crystallogr.* **1999**, *32*, 837.

Frequency calculations at the same level of theory have also been performed to identify all stationary points as minima (zero imaginary frequency). The effective core potentials (ECPs) of Hay and Wadt with a double- ζ valence basis sets (LanL2DZ)²⁷ were used to describe Mo, W, P, and S atoms, while the standard 6-31G basis set was used for C, O, and H atoms. Polarization functions ($\zeta(d) = 0.421$)²⁸ were added for S and for P ($\zeta(d) = 0.34$).²⁸ All the calculations were performed with the Gaussian 98 software package.²⁹

Acknowledgment. The National Science Council of the Republic of China and Academia Sinica financially supported this work.

Supporting Information Available: Tables of experimental data, selected bond distances and bond angles, and Mo_{ter}–S bond distances for a few mononuclear and binuclear molybdenum complexes and tables of atomic coordinates, isotropic and anisotropic displacement parameters, and all bond distances and angles for **4a–d**, **5a–d**, **6a,b,d**, **7**, and **8** with ORTEP drawings; these data are also available in electronic form as CIF files. This material is available free of charge via the Internet at <http://pubs.acs.org>.

OM050689M

(26) (a) Becke, A. D. *J. Chem. Phys.* **1993**, *98*, 5648. (b) Michlich, B.; Savin, A.; Stoll, H.; Preuss, H. *Chem. Phys. Lett.* **1989**, *157*, 200. (c) Lee, C.; Yang, W.; Parr, G. *Phys. Rev. B* **1988**, *37*, 785.

(27) Hay, P. J.; Wadt, W. R. *J. Chem. Phys.* **1985**, *82*, 299.

(28) Huzinaga, S. *Gaussian Basis Sets for Molecular Calculations*; Elsevier: Amsterdam, 1984.

(29) Frisch, M. J.; Trucks, G. W.; Schlegel, H. B.; Scuseria, G. E.; Robb, M. A.; Cheeseman, J. R.; Zakrzewski, V. G.; Montgomery, J. A., Jr.; Stratmann, R. E.; Burant, J. C.; Dapprich, S.; Millam, J. M.; Daniels, A. D.; Kudin, K. N.; Strain, M. C.; Farkas, O.; Tomasi, J.; Barone, V.; Cossi, M.; Cammi, R.; Mennucci, B.; Pomelli, C.; Adamo, C.; Clifford, S.; Ochterski, J.; Petersson, G. A.; Ayala, P. Y.; Cui, Q.; Morokuma, K.; Malick, D. K.; Rabuck, A. D.; Raghavachari, K.; Foresman, J. B.; Cioslowski, J.; Ortiz, J. V.; Stefanov, B. B.; Liu, G.; Liashenko, A.; Piskorz, P.; Komaromi, I.; Gomperts, R.; Martin, R. L.; Fox, D. J.; Keith, T.; Al-Laham, M. A.; Peng, C. Y.; Nanayakkara, A.; Gonzalez, C.; Challacombe, M.; Gill, P. M. W.; Johnson, B. G.; Chen, W.; Wong, M. W.; Andres, J. L.; Head-Gordon, M.; Replogle, E. S.; Pople, J. A. *Gaussian 98*, revision A.9; Gaussian, Inc.: Pittsburgh, PA, 1998.